The 17th International Conference on Motion and Vibration & The 20 th Asia-Pacific Vibration Conference
MoViC2024 & APVC2024

The crack location index for crack detection of a beam

Yusuke Mochida and Xutao Sun
School of Engineering, The University of Waikato
Private Bag 3105, Hamilton, 3240, New Zealand
E-mail: yusuke.mochida@waikato.ac.nz

Abstract
This study introduces a new index to be used for crack detection on a beam like structure. Our recent numerical modelling found sudden shifts in structural natural frequencies as a body with rotary inertia roving on a structure's surface passes a crack. Theoretically, this phenomenon made it possible to locate the crack by observing the abrupt frequency change from the curve of natural frequency versus mass location. In practice, the mass is located at discrete positions thus the curve of natural frequency is not continuous. This led to the consideration of Δf and $\Delta(\Delta f)$, where Δf is the natural frequency change when the mass is located in two adjacent positions and $\Delta(\Delta f)$ is the change of Δf. The plots of Δf or $\Delta(\Delta f)$ against mass location show peaks at the crack location and they could be highlighted. However, further study shows that the plots of Δf or $\Delta(\Delta f)$ sometimes give false peaks, which makes it challenging to pinpoint the crack location This study aims to introduce a more robust index than $\Delta(\Delta f)$ that can suppress some of the false peaks, and hence the resulting curve can be more suitable for crack detection. We name it the crack location index. The crack location index was devised based on the participation of modal data in the expressions of natural frequency of a beam carrying a roving mass with rotary inertia and its derivative. They were demonstrated to be good candidates for locating the crack. The crack location index was applied to a numerical example of beam with a crack, and the crack location was pinpointed. It was shown that there were fewer false peaks in the curve of the crack location index than that of $\Delta(\Delta f)$.

Keywords : Crack location index, Crack detection, Beam, Vibration, Natural frequency, Roving mass

1. Introduction

The recent research (Cannizzaro, 2018, Ilanko, et al, 2017, 2018, 2019) found sudden shifts in structural natural frequencies as a body with rotary inertia roving on a structure's surface passes a crack. Theoretically, this phenomenon made it possible to locate the crack by observing the abrupt frequency change from the curve of natural frequency (f) versus mass location. However, in practice, the mass is located at discrete positions thus the curve of natural frequency is not continuous. With a large step size, the change in the magnitude of the natural frequency between two adjacent mass location (Δf) increases and the crack location can be less observable from the curves of some natural frequencies. This led to the consideration of $\Delta(\Delta f)$, which is the change of Δf. The plots of $\Delta(\Delta f)$ against mass location show peaks at the crack location and they could also be used in crack detection of a structure if plotting Δf only does not show clear crack location.

Even though they exhibit potential in crack detection, further study (Sun, 2023) shows that the plots of Δf or $\Delta(\Delta f)$ sometimes give false peaks as the change in the natural frequencies also depend on the magnitude of roving step size and the mode shape. This makes it difficult to find the crack location. This study aims to introduce a more robust index (Crack Location Index) than Δf or $\Delta(\Delta f)$ that can suppress some of the false peaks, and hence the resulting curve can be more suitable for crack detection.

2. Theoretical Derivation

The crack location index is devised based on the participation of modal data in the expressions of natural frequency

of a beam carrying a roving mass with rotary inertia and its derivative. We consider an Euler-Bernoulli beam carrying a mass with rotary inertia as shown in Fig. 1.

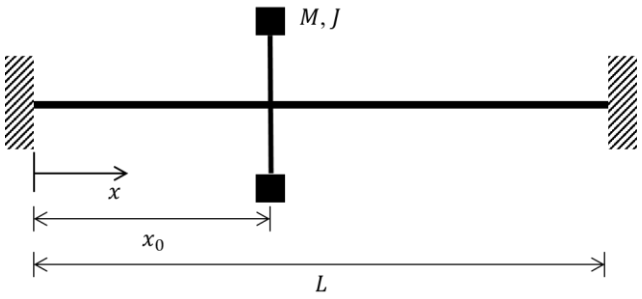

Fig. 1 A beam carrying a roving mass with rotary inertia.

The m^{th} natural frequency of the intact beam carrying a mass at x can be approximated using the following equation (Sun, 2023).

$$\omega_m^2(x) = \frac{\omega_{bm}^2}{1 + \dfrac{M\phi_m^2(x) + J\phi_m(x)\phi_m'(x)}{\bar{m}\psi_m}} \tag{1}$$

where $\bar{\boldsymbol{m}}$ is mass per unit length, $\phi_m(x)$ is the m^{th} mode shape of the beam, ω_{bn} is the m^{th} natural frequency of the bare beam (i.e. the beam without carrying a mass). The prime represents the derivative with respect to x. M and J donate the translational inertia and rotary inertia of the mass, respectively. ψ_m is the integral of the product of m^{th} mode shapes evaluated over the beam length.

From Eq. (1), ω_m is directly relevant to the natural frequency of the bare beam and the modal data $\boldsymbol{\phi_m}(x)$ and $\phi_m'(x)$ of the bare beam at the mass location. It can be seen that the presence of M and J reduces ω_m. M is involved by multiplying the mode shape squared at the mass location, while J is engaged by multiplying the mode shape and modal slope at the mass location. The expression of the natural frequency change due to the mass location can be found by taking the first derivative of ω_m with respect to mass location.

$$\frac{d\omega_m(x)}{dx} = \frac{\omega_m\sqrt{\bar{m}\psi_m}[M\phi_m(x)\phi_m'(x) + J\phi_m'^2(x) + J\phi_m(x)\phi_m''(x)]}{[\bar{m}\psi_m + M\phi_m^2(x) + J\phi_m(x)\phi_m'(x)]^{3/2}} \tag{2}$$

From Eq. (2), apart from mode shape and modal slope, $\frac{d\omega_m(x)}{dx}$ is also relevant to $\phi_m''(x)$ i.e. the modal curvature of the bare beam at the mass location. As $\phi_m(x)$, $\phi_m'(x)$, $\phi_m''(x)$ are not independent of each other, it is impossible to deduce the extrema of ω_m and $\frac{d\omega_m(x)}{dx}$ directly from the extrema of $\phi_m(x)$, $\phi_m'(x)$, $\phi_m''(x)$. However, the involvement of modal data in the expressions of ω_m and $\frac{d\omega_m(x)}{dx}$ provides some insights for devising the crack location index, and examining the relevance between the modal data of the intact bare beam and the natural frequency data of the cracked beam carrying a roving mass led the crack location index ζ.

When the coordinate of the mass location is x_0, the crack location index for the m^{th} mode at x_0, i.e. $\zeta_m(x_0)$, is expressed as

$$\zeta_m(x_0) = \Delta(\Delta f_m)|_{x_0} \cdot \phi_m'(x_0) \cdot \phi_m'''(x_0) \tag{3}$$

where $\Delta(\Delta f)|x_0$ is the change of frequency shift of the m^{th} natural frequency when the mass is located at x_0. $\phi_m'(x)$ and $\phi_m'''(x)$ are the modal slope and the derivative of modal curvature of the intact bare beam (i.e. the intact beam without carrying a mass) evaluated at x_0, respectively.

3. Numerical Examples

As an example, we considered a clamped-clamped beam whose length 623 mm with a crack at 394mm from its

end. The curves of f, $\Delta(\Delta f)$, and ζ versus mass location for the third mode are shown in Fig. 2. The extrema of the curve of f correspond to the peaks in the curve of $\Delta(\Delta f)$. Therefore, multiplying $\Delta(\Delta f)$ by the derivative of mode shape (i.e. $\phi_m'(x)$) and the derivative of modal curvature (i.e. $\phi_m'''(x)$) would help suppress the peaks in the curve of $\Delta(\Delta f)$. As shown in the curve of ζ, there are less peaks compared with the curve of $\Delta(\Delta f)$.

By observing other modes, it was found that the crack location becomes more and more visible in the curve of ζ as the mode number drops. The crack location can be clearly seen in the curves of ζ of the first three modes because there is no false peaks except where near the boundaries. The curve of f reaches extrema when the mass is located near boundaries possibly due to the contribution of large $\phi_m'(x)$, and the resulting peaks in the curve of $\Delta(\Delta f)$ cannot be suppressed using the current crack location index. Therefore, the crack location index is most effective for the first three modes excluding regions near boundaries.

By intercepting the results from 0.1m to 0.5m, the regions near boundaries are excluded. The resulting curves of ζ for the first three modes are shown in Fig. 3. From Fig. 3, the location of the crack can be pinpointed from the curves of the crack location index ζ_m.

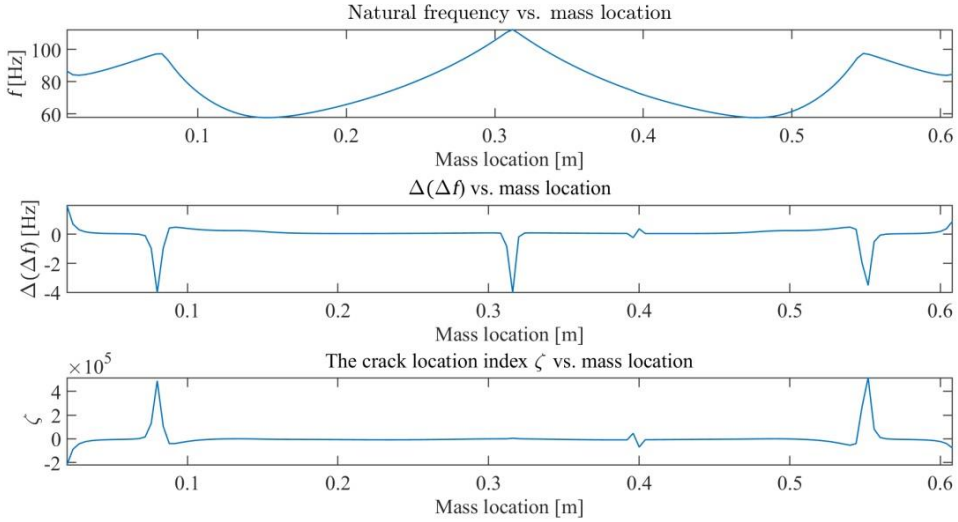

Fig. 2 The natural frequency data and the crack location index, ζ of the 3rd mode of the clamped-clamped beam carrying a roving mass with a crack

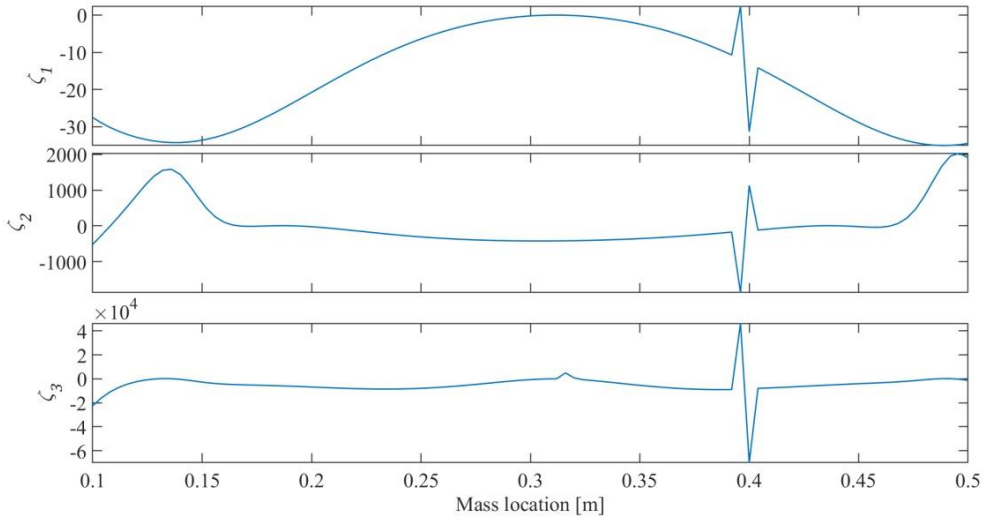

Fig. 3 The curves of the crack location indices, ζ_1, ζ_2 and ζ_3, excluding regions near boundaries.

3.1 Different Crack Locations

In this section, the crack is positioned near the extreme points of the second and third mode shapes of the

undamaged bare beam. In those situations, when the mass passes the crack, $\phi'_m(x_0)$ approaches zero and $\zeta_m(x_0)$ tends towards zero as shown in Eq. (3). Consequently, the crack location cannot be indicated by the curve of ζ_m. However, by utilizing the second and third modes for crack detection, it is anticipated that when the crack is situated near an extreme point of the second mode shape of the intact bare beam, $\zeta_2(x_0)$ approaches zero when the mass passes the crack but $\zeta_3(x_0)$ still gives the crack location and vice versa.

In the first scenario, the crack is located at $0.442m$, causing $\phi'_2(x_0)$ to approach zero as the mass passes the crack. The corresponding plots of ζ for the first three modes, excluding regions near the boundaries, are depicted in Fig.4. Observing the figure, ζ_2 yields inconclusive outcomes as the peak induced by the mas passing the crack is also suppressed. However, the peak in the curve of ζ_3 remains unaffected and the crack location is still visible.

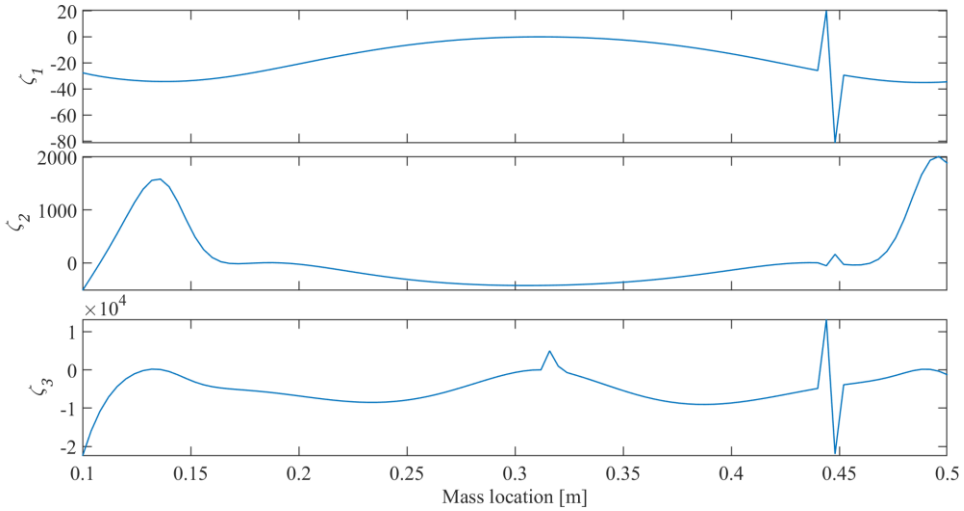

Fig. 4 The curves of the crack location indices $\boldsymbol{\zeta_1}$, $\boldsymbol{\zeta_2}$, and $\boldsymbol{\zeta_3}$ excluding regions near boundaries (crack location: $0.442\boldsymbol{m}$).

In the second scenario, the crack is located at $0.486m$ causing $\phi'_3(x_0)$ to approach zero as the mass passes the crack. The resulting curves of ζ for the first three modes, excluding the regions near boundaries are shown in Fig 5. From the figure, there is no obvious peak in the curve of ζ_3 except for a small peak in the middle of the beam. The small peak is the residue of the suppression of a large peak. The crack location can still be pinpointed from the curve of ζ_2. In general, using both ζ_2 and ζ_3 ensures that the crack location is always visible in the curve of ζ. Even if the peak caused by the mass passing the crack is suppressed in one curve, it invariably persists in the other.

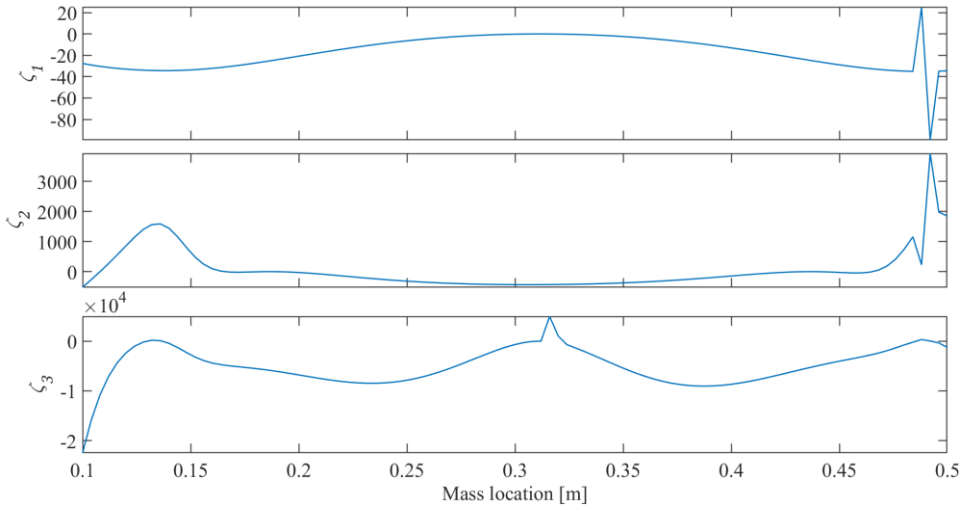

Fig. 5 The curves of the crack location indices $\boldsymbol{\zeta_1}$, $\boldsymbol{\zeta_2}$, and $\boldsymbol{\zeta_3}$ excluding regions near boundaries (crack location: $0.486\boldsymbol{m}$).

3.2 Different Boundary Conditions

The crack location index is applied to cracked beams with different boundary conditions. Fig. 6 shows the curves of ζ_1, ζ_2, and ζ_3 for the beams with cracks under simply supported, clamped-pinned, and clamped-free conditions, respectively. The crack is located at $0.394m$. Despite alterations in boundary conditions, the curves of ζ_2 and ζ_3 consistently exhibit a distinct shift when the mass passes the crack, thus the crack location can be pinpointed.

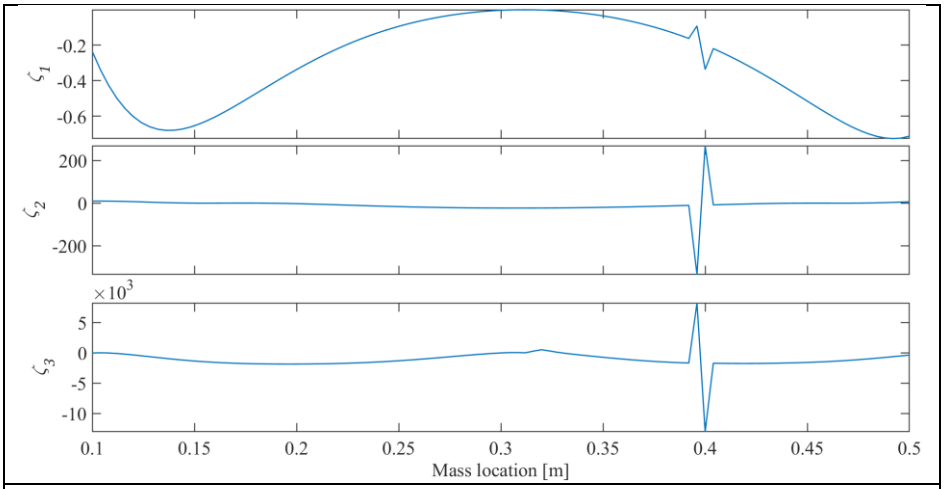

(a) simply-supported beam

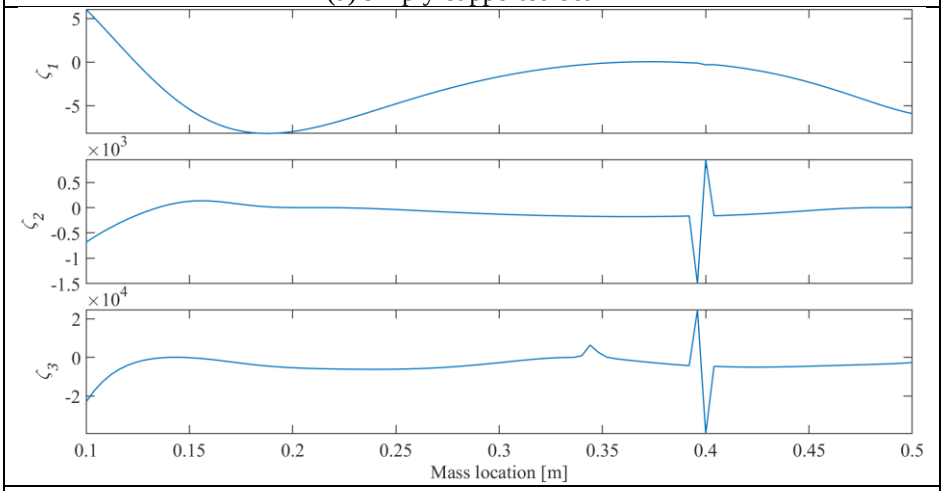

(b) clamped-pinned beam

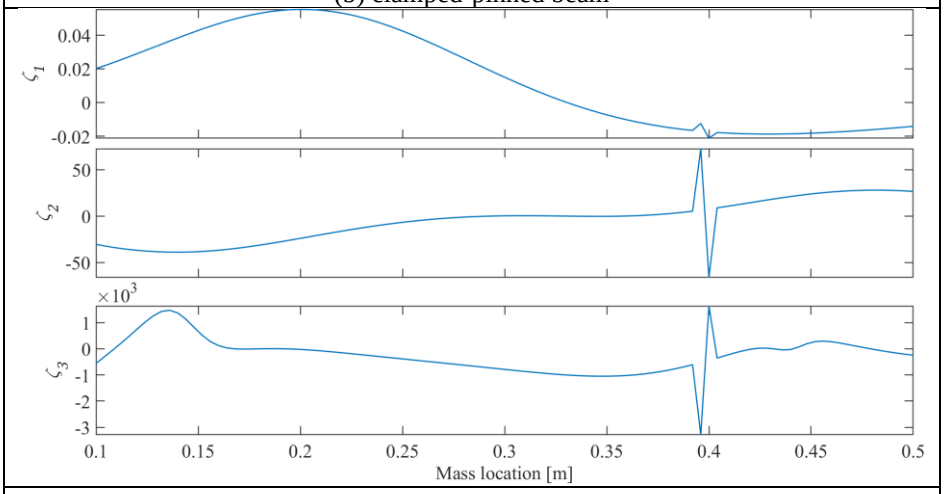

(c) cantilever beam

Fig. 6 The curves of $\boldsymbol{\zeta_1}$, $\boldsymbol{\zeta_2}$, and $\boldsymbol{\zeta_3}$ for different boundary conditions (regions near boundaries are excluded).

4. Discussions

The numerical example demonstrates a robust methodology for crack detection in beams using modal analysis and the crack location index (ζ). By examining the frequency (f), the difference of frequency change ($\Delta(\Delta f)$), and the crack location index (ζ) across different modes and boundary conditions, the study shows that multiplying $\Delta(\Delta f)$ with the derivatives of the mode shape and modal curvature helps suppress unwanted peaks, making the crack location more distinguishable. For the first three modes, the crack is clearly identifiable away from the boundaries, with fewer false peaks.

In scenarios where the crack is near the extreme points of the second and third mode shapes, the reliability of using multiple modes ensures that the crack location is always detectable. This method proves effective across various boundary conditions, highlighting its versatility and robustness in structural health monitoring. However, to validate these theoretical observations, experimental studies are necessary. Conducting experiments will help verify the accuracy and reliability of the crack detection method, ensuring its practical applicability in structural health monitoring.

5. Conclusions

The crack location index ζ_m was devised by incorporating modal data into the expressions of ω_m and $\frac{d\omega_m(x)}{dx}$. This index was then applied to numerical examples with different crack positions and boundary conditions, pinpointing the crack location. It was shown that the curve of the crack location index exhibited fewer false peaks compared to $\Delta(\Delta f)$. Furthermore, the first three crack location indices, ζ_1, ζ_2 and ζ_3 were demonstrated to be good candidates for locating the crack.

References

Cannizzaro, F., De Los Rios, J., Caddemi, S., Calio, I., and Ilanko, S., 'On the use of a roving body with rotary inertia to locate cracks in beams', Journal of Sound and Vibration, 425, 275-300, (2018)

Ilanko, S., De Los Rios, J., Caddemi, S., and Kennedy, D., 'The effect of roving rotary inertia as it passes a crack', ISVCS 2017 – Proceedings of 11th International Symposium on Vibrations of Continuous Systems, 34-37, (2017).

Ilanko, S.; Mochida, Y., and De Los Rios, J., 'Vibration analysis of cracked structures as a roving body passes a crack using the Rayleigh-Ritz Method', EPI International Journal of Engineering, 1, pp. 30-34, (2018).

Ilanko, S.; Mochida, Y., De Los Rios, J., and Kennedy, D., 'Separating the effect of crack severity and location in a skeletal structure with a single crack', ISVCS 2019 – Proceedings of 12th International Symposium on Vibrations of Continuous Systems, (2019).

Sun, X., 'Theoretical and Experimental Investigation on Natural Frequency-based Crack Detection'. PhD Thesis, The University of Waikato, 2023.